Thermal Spreading Resistance in Ballistic-Diffusive Regime of Wide-Bandgap Semiconductors

Yang Shen

Department of Engineering Mechanics, School of Aerospace Engineering, Tsinghua University

November 3, 2021

Overview

- Under gray-media approximation, Dr.Hua developed a semi-empirical thermal resistance model which could consider the influence of both thermal spreading and ballistic effects.
- Whereas real semiconductor materials like GaN exhibit an extremely broad distribution of phonon MFPs, the validity of the model needs to be further verified.
- We inspected the model-predicted thermal spreading resistance by Phonon Monte Carlo simulations with the phonon dispersion of various typical semiconductor materials. Based on the analyses of deviations, the model was further revised and generalized.

Outline

Wide Bandgap Semiconductors

- Wide bandgap (WBG) semiconductors like GaN HEMTs, SiC MESFETs, and recently burgeoning untra-WBG β-Ga_2O_3 based devices, show excellent electronic properties.
- Whereas owing to their super high power density, the actural performance is largely restricted by the significant over-heating within the device.
- Heat generation is extremely localized at the top of the channel layer, which results in a near-junction temperature spike, or so-called ”hot-spot”.

Thermal Spreading

Thermal spreading resistance occurs when heat enters the system through a small region and is transferred by conduction to a larger region or heat sink.

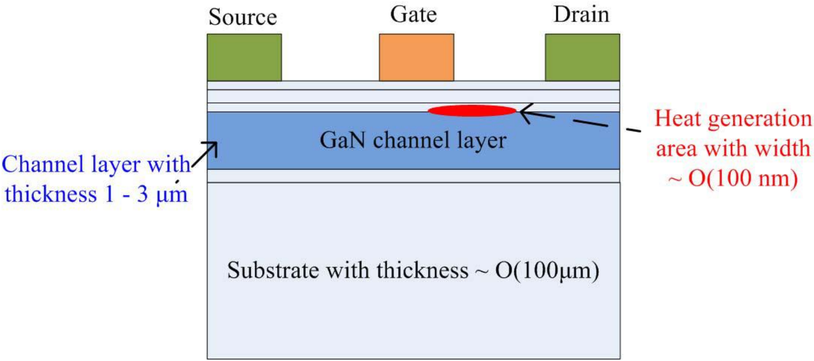

Figure 1: Typical structure of GaN HEMTs.

Thermal Spreading Resistance Model

Thermal spreading resistance models have been extensively studied based on Fourier's heat conduction law,[1]

$$\theta_j\left(x, y, z_j\right) =$$

$$A_{0j} + B_{0j}z + \sum_{m=1}^{\infty} \cos\left(\lambda_m x\right)\left[A_{1j}\cosh\left(\lambda_m z_j\right) + B_{1j}\sinh\left(\lambda_m z_j\right)\right]$$

$$+ \sum_{n=1}^{\infty} \cos\left(\delta_n y\right)\left[A_{2j}\cosh\left(\delta_n z_j\right) + B_{2j}\sinh\left(\delta_n z_j\right)\right]$$

$$+ \sum_{m=1}^{\infty}\sum_{n=1}^{\infty} \cos\left(\lambda_m x\right)\cos\left(\delta_n y\right)\left[A_{3j}\cosh\left(\beta_{mn} z_j\right) + B_{3j}\sinh\left(\beta_{mn} z_j\right)\right]$$

Current models don't take ballistic effects into account.

[1] Y. Muzychka, J. Culham, and M. Yovanovich, "Thermal spreading resistance of eccentric heat sources on rectangular flux channels," *J. Electron. Packag.*, vol. 125, no. 2, pp. 178–185, 2003.

Problem Statement

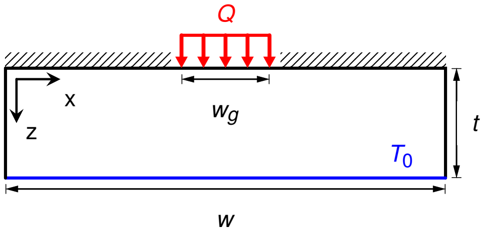

Figure 2: Schematic for the basic system in a single period.

The geometry of the system can be characterized by:

$$w_g/w \quad \text{and} \quad w/t$$

Two Knudsen numbers, Kn_t and Kn_w, were defined to characterize the strength of ballistic effects,

$$Kn_t = l_0/t, \quad Kn_w = l_0/w_g$$

Thermal Resistance Model[2] - Decoupling

Thermal spreading part

Cross-plane ballistic part

Heat source ballistic part

$$\frac{R_t}{R_{1d\_0}} = \frac{R_F}{R_{1d\_0}} \cdot \frac{R_{1d}}{R_{1d\_0}} \cdot \left[\frac{R_t}{R_{1d}}\left(\frac{R_F}{R_{1d\_0}}\right)^{-1}\right]$$

$$\frac{R_F}{R_{1d\_0}} = 1 + (\frac{w}{w_g})^2(\frac{w}{t})\sum_{n=1}^{\infty}\frac{8\sin^2\left(\frac{w_g n\pi}{2w}\right) * \cos^2(\frac{n\pi}{2})}{(n\pi)^3\coth(\frac{tn\pi}{w})}$$

$$\frac{R_{1d}}{R_{1d\_0}} = 1 + 2/3Kn_t$$

$$\frac{R_t}{R_{1d}}\left(\frac{R_F}{R_{1d\_0}}\right)^{-1} = r_w = 1 + A_w\left(w_g/w, w/t\right)Kn_w$$

[2] Y.-C. Hua, H.-L. Li, and B.-Y. Cao, “Thermal spreading resistance in ballistic-diffusive regime for gan hemts,” *IEEE Transactions on Electron Devices*, vol. 66, no. 8, pp. 3296–3301, 2019.

Effective Thermal Conductivity

Ballistic effects can be represented by the degradation of the effective thermal conductivity of nanostructures,

$$R_t = R_F(k_{eff})$$
$$\frac{k_{eff}}{k_0} = \frac{1}{\left(1 + A_w\left(w_g/w, w/t\right) Kn_w\right)\left(1 + \frac{2}{3}Kn_t\right)}$$

The degradation of the effective thermal conductivity is caused by the suppression of mean free paths of phonons,

$$k_{eff} = \frac{1}{3}\sum_j \int_0^{\omega_j} \hbar\omega \frac{\partial f_0}{\partial T}\,\mathrm{DOS}_j(\omega) v_{g\omega j} l_{j,m} \mathrm{d}\omega$$
$$l_{j,m} = \frac{l_{0,j}}{\left(1 + A_w\left(w_g/w, w/t\right) Kn_{w\_\omega,j}\right)\left(1 + \frac{2}{3}Kn_{t\_\omega,j}\right)}$$

MFP Distribution of Real Semiconductor Materials

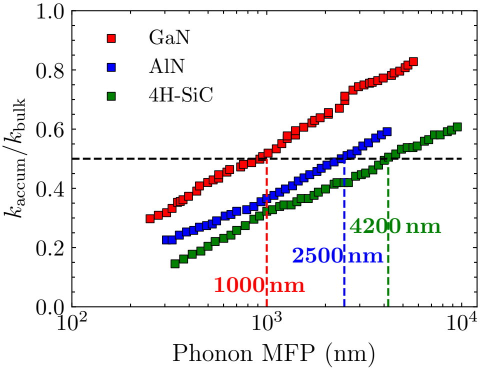

Figure 3: Normalized thermal conductivity accumulation functions of GaN, AlN, and 4H-SiC at temperatures near 300 K as a function of phonon MFP.[3]

[3] J. P. Freedman, J. H. Leach, E. A. Preble, *et al.*, "Universal phonon mean free path spectra in crystalline semiconductors at high temperature," *Scientific reports*, vol. 3, no. 1, pp. 1–6, 2013.

This Work

Motivation

- When faced with such a broad distribution of phonon MFPs, could the model still keep valid and address the thermal spreading and ballistic effects well?

This Work

- Dispersion Phonon Monte Carlo simulations were conducted to verify the reliability of the model, and the model was further revised based on analyses of deviations between the results.
- The thermal resistance and temperature distributions predicted by MC simulations and FEM with the effective thermal conductivity were compared, which illustrates the practicability of our model.

Phonon Dispersion

- An isotropic sine-shaped phonon dispersion (Born-von Karman dispersion) is used.
- Longitudinal and transverse branches are not differentiated.

$$\omega(k) = \omega_{\max} \sin\left(\pi k / 2k_m\right)$$

$$k_m = \left(\frac{6\pi^2 N}{V}\right)^{1/3}, \ a = \pi / k_m, \ \omega_m = 2v_{0g}/a$$

Relaxation time

Matthiessen's rule:

$$\tau^{-1} = \tau_{impurity}^{-1} + \tau_U^{-1} = A\omega^4 + B\omega^2 T \exp(-C/T)$$

Thermal conductivity fitting:

$$\mathscr{L}(A, B, C) = \sum \left\| \frac{1}{3} \sum_p \int_0^{\omega_m} C_\omega v_\omega l_\omega \mathrm{d}\omega - k_{exp} \right\|^2$$

$$C(\omega, p) = \hbar\omega D(\omega, p) \frac{\partial f^{BE}}{\partial T} = \hbar\omega \frac{\kappa^2}{2\pi^2 \left| v_g \right|} \frac{\hbar\omega e^{\frac{\hbar\omega}{Tk_B}}}{T^2 k_B \left(e^{\frac{\hbar\omega}{Tk_B}} - 1 \right)^2}$$

Phonon Dispersion and Relaxation time

Parameter (Unit)	GaN	AlN	SiC	β-Ga_2O_3
$k_0\,(1 \times 10^9\,\mathrm{m}^{-1})$	10.94	11.19	8.94	6.74
$\omega_m\,(1 \times 10^{13}\,\mathrm{rad/s})$	3.50	5.18	7.12	1.6
a_D (Å)	2.87	2.81	3.51	4.66
$A\,(1 \times 10^{-45}\,\mathrm{s}^3)$	5.26	10.5	1.00	1.38E-6
$B\,(1 \times 10^{-19}\,\mathrm{s/K})$	1.10	0.728	0.596	9.31
C (K)	200	287.5	235.0	62.6

Table 1: Fitted phonon dispersion and scattering parameters for typical WBG semiconductors[4]. For β-Ga_2O_3, thermal conductivity along [100] crystallographic direction was used to fit the parameters.

[4] Q. Hao, H. Zhao, and Y. Xiao, "A hybrid simulation technique for electrothermal studies of two-dimensional gan-on-sic high electron mobility transistors," *Journal of Applied Physics*, vol. 121, no. 20, p. 204 501, 2017.

Energy-based Variance-reduced Monte Carlo

When considering phonon dispersion, the main difference is that phonon bundles emitted from phonon baths will have different properties, and their properties will be redetermined after phonon–phonon scattering[5].

Emitting Sampling

$$W_{\mathrm{ph-bnd}} = \frac{C_{p,\omega} v_{p,\omega}}{\sum_p \int_\omega C_{p,\omega} v_{p,\omega} \mathrm{d}\omega} \mathrm{d}\omega$$

Scattering Sampling

$$W_{\mathrm{ph-ph}} = \frac{C_{p,\omega} v_{p,\omega} / l_{p,\omega}}{\sum_p \int_\omega \left(C_{p,\omega} v_{p,\omega} / l_{p,\omega} \right) \mathrm{d}\omega} \mathrm{d}\omega$$

---

[5] H.-L. Li, J. Shiomi, and B.-Y. Cao, "Ballistic-diffusive heat conduction in thin films by phonon monte carlo method: Gray medium approximation versus phonon dispersion," *Journal of Heat Transfer*, vol. 142, no. 11, p. 112 502, 2020.

Total Thermal Resistance

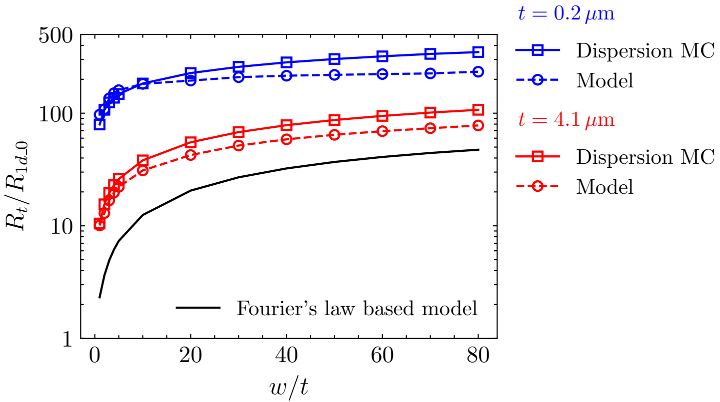

Figure 4: Dimensionless total thermal resistance of GaN as a function of w/t with $w_g/w = 0.01$ under different thickness.

Analysis of Deviations

$$k_{eff} = \frac{1}{3}\sum_j \int_0^{\omega_j} \hbar\omega \frac{\partial f_0}{\partial T} \mathrm{DOS}_j(\omega) v_{g\omega j} l_{j,m} \mathrm{d}\omega$$

$$l_{j,m} = \frac{l_{0,j}}{\left(1 + A_w\left(w_g/w, w/t\right) Kn_{w\_\omega,j}\right)\left(1 + \frac{2}{3} Kn_{t\_\omega,j}\right)}$$

Decoupling of Different Ballictic Effects

- The deviation is mainly caused by the insufficiency of the model to reflect ballistic effects due to broad phonon MFP distributions.
- The key issue here is to decouple the effects of cross-plane ballistic part and heat-source ballistic part.

Elimination of Heat-Source Ballistic Part

Original model,

$$k_{eff} = \frac{1}{3}\sum_j \int_0^{\omega_j} \hbar\omega \frac{\partial f_0}{\partial T} \mathrm{DOS}_j(\omega) v_{g\omega j} l_{j,m} \mathrm{d}\omega$$

$$l_{j,m} = \frac{l_{0,j}}{\left(1 + A_w\left(w_g/w, w/t\right) Kn_{w\_\omega,j}\right)\left(1 + \frac{2}{3} Kn_{t\_\omega,j}\right)}$$

Model 1: Substitute $\left(1 + A_w\left(w_g/w, w/t\right) Kn_{w\_\omega,j}\right)$ with r_w directly calculated from the results of Dispersion Monte Carlo,

$$k_{eff} = \frac{1}{3}\sum_j \int_0^{\omega_j} \hbar\omega \frac{\partial f_0}{\partial T} \mathrm{DOS}_j(\omega) v_{g\omega j} l_{j,m} \mathrm{d}\omega$$

$$l_{j,m} = \frac{l_{0,j}}{\left(r_{w,\mathrm{dispersion}}\right)\left(1 + \frac{2}{3} Kn_{t\_\omega,j}\right)}$$

Total Thermal Resistance of Model 1

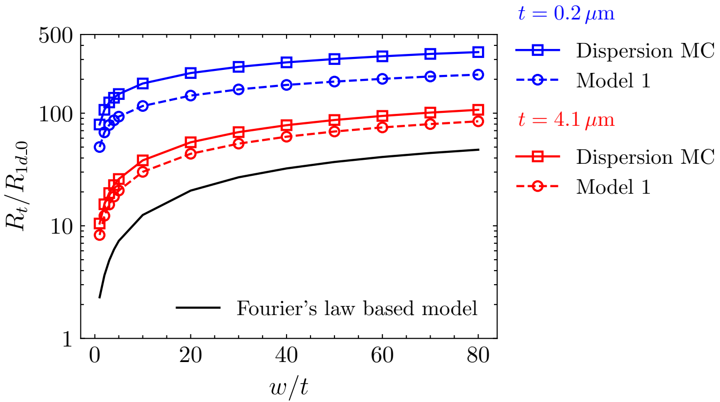

Figure 5: Dimensionless total thermal resistance of GaN as a function of w/t with $w_g/w = 0.01$ under different thickness.

Weighted Average of Modal Phonon MFPs

The Average phonon MFP could be extracted by employing Majumdar's model for cross-plane heat conduction to calculate $F(j,\omega)$ and fit the dispersion results.

$$k_{\text{eff}}/k_{\text{bulk}} = \frac{1}{3}\sum_{j}\int_{0}^{\omega_j} \hbar\omega \frac{\partial f_0}{\partial T}\,\text{DOS}_j(\omega) v_{g\omega j} F(j,\omega)\mathrm{d}\omega/k_{\text{bulk}}$$

$$= \frac{1}{1 + 4/3 \cdot l_{ave}/L}$$

Our previous studies demonstrated that this way to extract the phonon averate MFP could reflect the mode dependent MFP depression well[6].

[6] H.-L. Li, J. Shiomi, and B.-Y. Cao, "Ballistic-diffusive heat conduction in thin films by phonon monte carlo method: Gray medium approximation versus phonon dispersion," *Journal of Heat Transfer*, vol. 142, no. 11, p. 112 502, 2020.

Weighted Average of Modal Phonon MFPs

Material	Average MFP (nm)
GaN	1612.3
AlN	3401.4
SiC	2506.96
β-Ga_2O_3	450.7

Table 2: The average phonon MFP of different materials.

The average Knudsen numbers could be then defined to characterize the strength of the ballistic effects,

$$Kn_t = l_{ave}/t$$
$$Kn_w = l_{ave}/w_g$$

Dependence Analysis of r_{Kn_t}

$$r_{Kn_t} = R_{\text{MC}} / R_{\text{Model-1}}$$

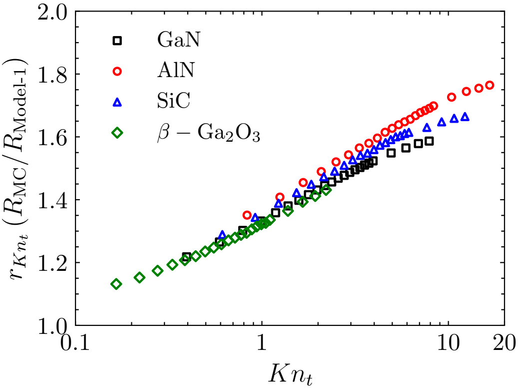

Figure 6: Thermal resistance ratio as a function of Kn_t of different materials.

Elimination of Cross-Plane Ballistic Part

Original model,

$$k_{eff} = \frac{1}{3}\sum_j \int_0^{\omega_j} \hbar\omega \frac{\partial f_0}{\partial T} \mathrm{DOS}_j(\omega) v_{g\omega j} l_{j,m} \mathrm{d}\omega$$

$$l_{j,m} = \frac{l_{0,j}}{\left(1 + A_w\left(w_g/w, w/t\right) Kn_{w\_\omega,j}\right)\left(1 + \frac{2}{3} Kn_{t\_\omega,j}\right)}$$

Model 2: Apply r_{Kn_t} to $l_{j,m}$,

$$k_{eff} = \frac{1}{3}\sum_j \int_0^{\omega_j} \hbar\omega \frac{\partial f_0}{\partial T} \mathrm{DOS}_j(\omega) v_{g\omega j} l_{j,m} \mathrm{d}\omega$$

$$l_{j,m} = \frac{l_{0,j}}{\left(1 + A_w\left(w_g/w, w/t\right) Kn_{w\_\omega,j}\right)\left(1 + \frac{2}{3} Kn_{t\_\omega,j}\right) r_{Kn_t}}$$

Total Thermal Resistance of Model 2

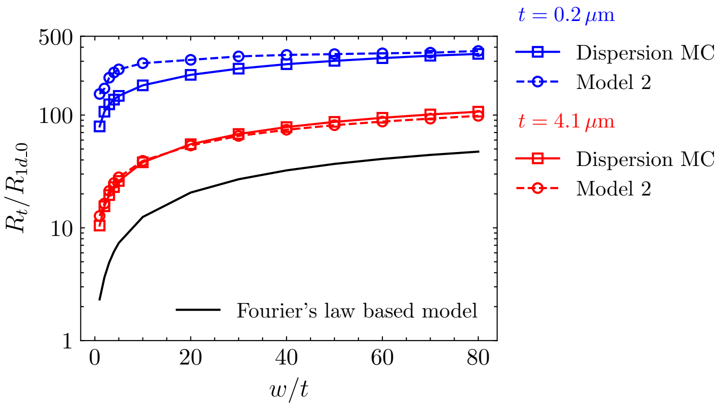

Figure 7: Dimensionless total thermal resistance of GaN as a function of w/t with $w_g/w = 0.01$ under different thickness.

$$Kn_w = \frac{l_0}{(w_g/w) \cdot (w/t) \cdot t}$$

Dependence Analysis of r_{Kn_w}

$$r_{Kn_w} = R_{\mathrm{MC}} / R_{\text{Model-2}}$$

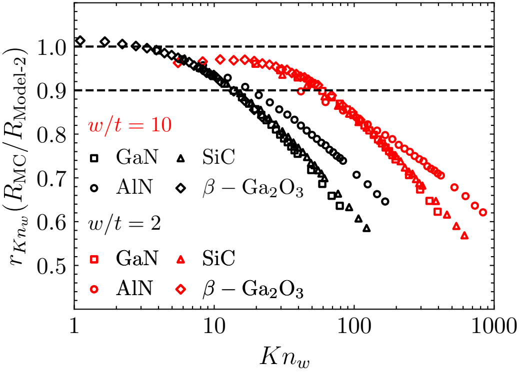

Figure 8: Thermal resistance ratio as a function of Kn_w.

Dependence Analysis

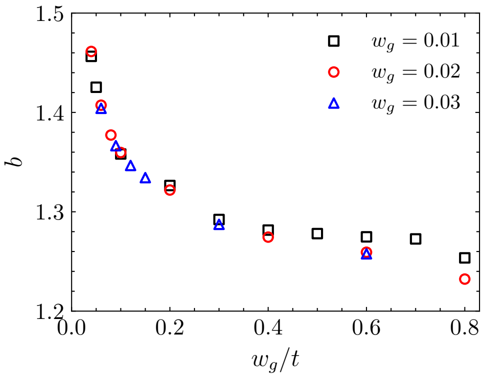

Figure 9: Fitting parameter b varying with w_g/t.

$$r_{Kn_w} = -0.17 \cdot \log(Kn_w) + b(w_g/t)$$

Revised Thermal Resistance Model

$$R_t = R_F(k_{\text{eff}})$$
$$k_{eff} = \frac{1}{3}\sum_j \int_0^{\omega_j} \hbar\omega \frac{\partial f_0}{\partial T} \text{DOS}_j(\omega) v_{g\omega j} l_{j,m} \mathrm{d}\omega$$
$$l_{j,m} = \frac{l_{0,j}}{\left(1 + A_w\left(w_g/w, w/t\right) Kn_{w\_\omega,j}\right)\left(1 + \frac{2}{3}Kn_{t\_\omega,j}\right) r_{Kn_t} r_{Kn_w}}$$

$$r_{Kn_t} = 0.15 \cdot \log(Kn_t) + 1.35$$
$$r_{Kn_w} = -0.17 \cdot \log(Kn_w) + b(w_g/t)$$
$$\frac{1}{1 + 4/3 \cdot l_{ave}/L} = \frac{1}{3}\sum_j \int_0^{\omega_j} \hbar\omega \frac{\partial f_0}{\partial T} \text{DOS}_j(\omega) v_{g\omega j} F(j,\omega) \mathrm{d}\omega / k_{\text{bulk}}$$

It should be noted that the revised thermal resistance model is still dispersion-independent.

Total Thermal Resistance

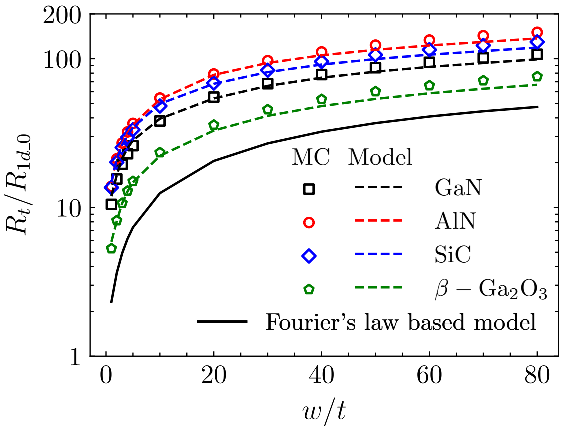

Figure 10: Dimensionless total thermal resistance of Different semiconductor materials as a function of w/t with $w_g/w = 0.01$ and $t = 2.7\,\mu m$.

Temperature Distribution

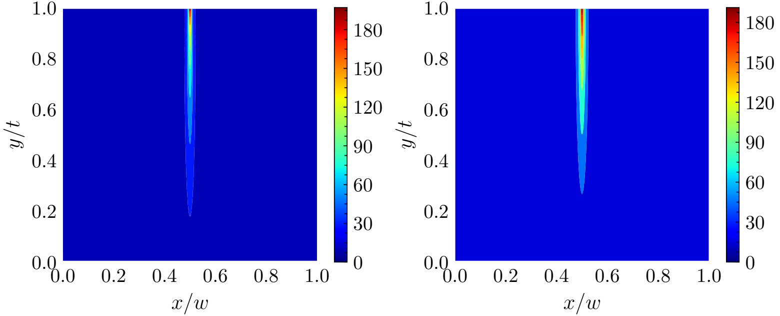

(a) Dispersion MC.

(b) FEM with k_{eff}.

Figure 11: Dimensionless temperature distributions by FEM with k_{eff} and Dispersion MC.

Temperature Distribution

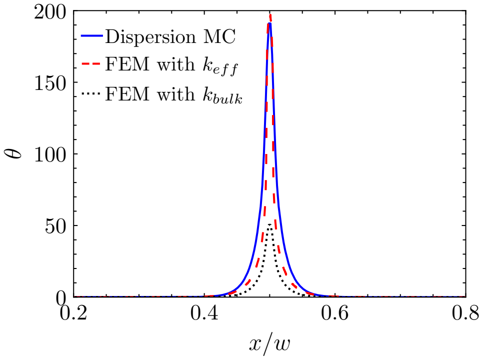

Figure 12: Temperature distribution at the top surface of the system.

FEM with effective thermal conductivity can give nearly the same peak temperature rise as that calculated by dispersion MC.

Computation Time

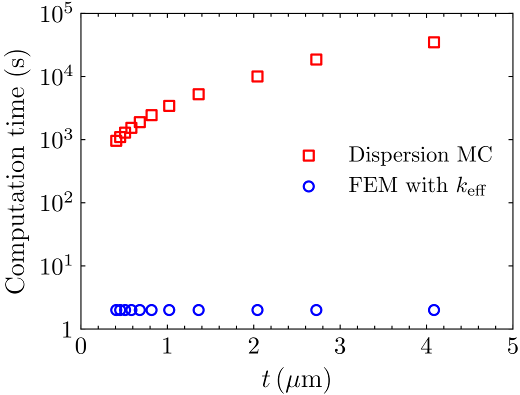

Figure 13: Computation time of Dispersion MC with 2×10^7 phonons and FEM with k_{eff} as a function of channel thickness using single core.

Conclusions

- We inspected the semi-empirical model with the phonon dispersion of several classical wide-bandgap semiconductor materials. It indicates that due to the broad phonon MFP distributions, there were deviations between the model predicted theramal resistance and those of Dispersion MC.
- The deviations could be characterized by the average Knudson number Kn_t, Kn_w, which refer to cross-plane and heat-source ballistic effects, respectively. The model was further revised to correct the deviations based on the analyses.
- Dimensionless temperature distributions by Dispersion Monte Carlo and FEM with effective thermal conductivity were compared, the results indicated that our model gave a highly efficient way to evaluate the thermal spreading and ballistic effects.

Thank You!